

Radiomics

Christian Salvatore
Scuola Universitaria Superiore IUSS Pavia

christian.salvatore@iusspavia.it

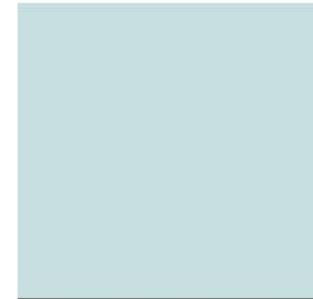
Radiomic hypothesis

Molecular heterogeneity of cancer lesions is cause of different clinical outcome.

Such heterogeneity can be captured, *in vivo*, on the entire lesion volume, by high-throughput quantitative radiomics descriptors from 3D image of cancer lesion.

Different expression level of a signature of radiomic features are able to predict different prognosis or treatment response of patients with similar cancer diagnosis (statistical analysis and predictive models).

Radiology



Robert J. Gillies, PhD
Paul E. Kinahan, PhD
Hedvig Hricak, MD, PhD, Dr(hc)

Radiomics: Images Are More than Pictures, They Are Data¹

In the past decade, the field of medical image analysis has grown exponentially, with an increased number of pattern recognition tools and an increase in data set sizes. These advances have facilitated the development of processes for high-throughput extraction of quantitative features that result in the conversion of images into mineable data and the subsequent analysis of these data for decision support; this practice is termed *radiomics*. This is in contrast to the traditional practice of treating medical images as pictures intended solely for visual interpretation. Radiomic data contain first-, second-, and higher-order statistics. These data are combined with other patient data and are mined

Radiomics: a new approach for the study of cancer



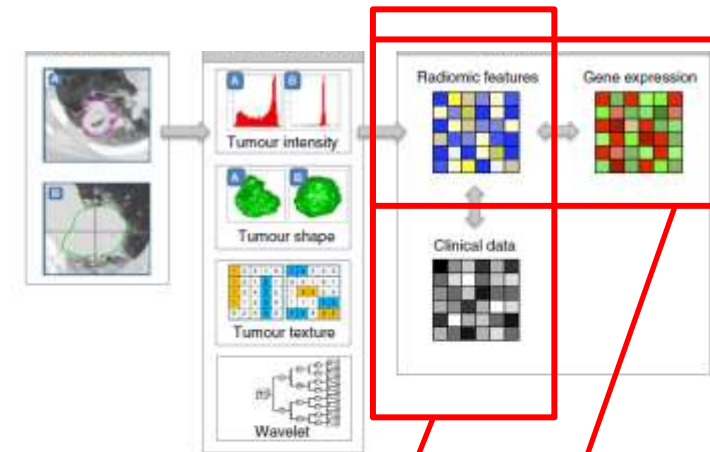
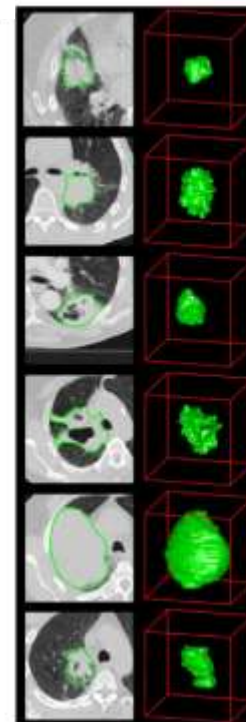
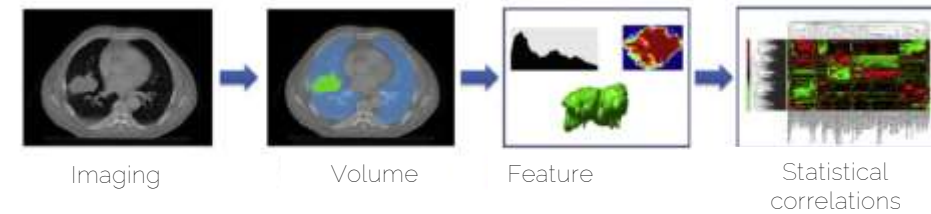
Published in final edited form as:
Eur J Cancer. 2012 March 14; 48(4): 441-446. doi:10.1016/j.ejca.2011.11.036.

Radiomics: Extracting more information from medical images using advanced feature analysis

Philippe Lambin^{a,*}, Emmanuel Rios-Velazquez^{a,c}, Ralph Leijenaar^{a,c}, Sara Carvalho^{a,c},
Ruud G.P.M. van Stiphout^{a,e}, Patrick Granton^{a,e}, Catharina M.L. Zegers^{a,e}, Robert Gillies^{b,e},
Ronald Boellard^{c,e}, André Dekker^{a,c}, and Hugo J.W.L. Aerts^{a,d,e}

^aDepartment of Radiation Oncology (MAASTRO), GROW – School for Oncology and Developmental Biology, Maastricht University Medical Center, Maastricht, The Netherlands ^bH. Lee Moffitt Cancer Center and Research Institute, Tampa, FL, USA ^cUniversity Medical Center, Department of Nuclear Medicine & PET Research, Amsterdam, The Netherlands ^dComputational Biology and Functional Genomics Laboratory, Department of Biostatistics and Computational Biology, Dana-Farber Cancer Institute, Harvard School of Public Health, USA

Comprehensive quantification
of disease phenotypes by
applying a large number of
quantitative image features
representing lesion
heterogeneity and correlating
with omics and clinical data

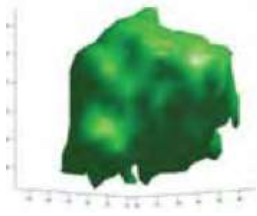
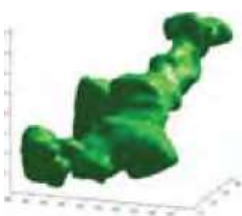
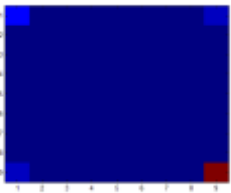
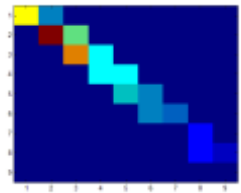
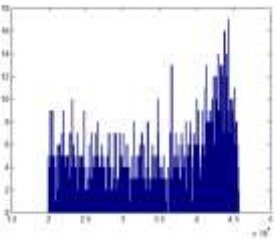
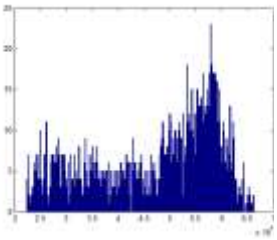
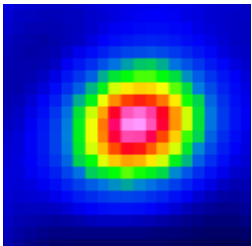
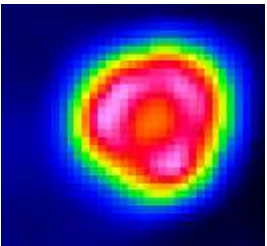


RADIOGENOMICS

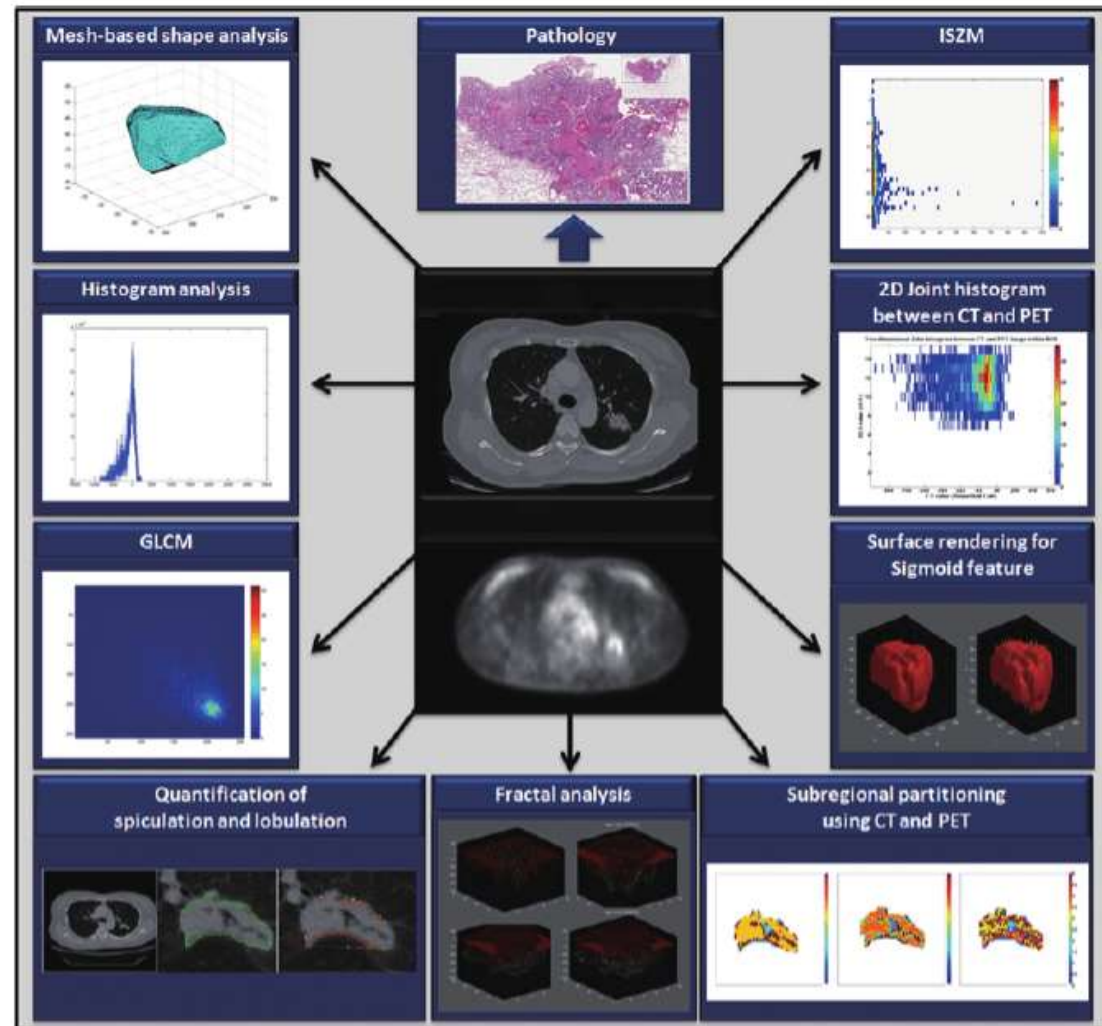
RADIOMICS

Texture and shape features

Feature	Description		Examples
Texture- First order	Grey level frequency distribution from histogram Analysis	Global	Minimum, mean and maximum intensity
			Standard deviation
			Skewness
			Kurtosis
			Percentile values
Texture- Second order	From spatial grey level dependence matrices (SGLDM) or co-occurrence matrices <i>They express how often a pixel of intensity i finds itself within a certain relationship to another pixel of intensity j</i>	Local	Range of intensities
			Entropy
			Energy
			Contrast
			Homogeneity
			Dissimilarity
			Uniformity
			Correlation
Texture- Third order	From neighbourhood grey-tone difference matrices (NGTDMs)	Local	Coarseness
			Contrast
			Busyness
			Complexity
	From voxel alignment matrices	Regional	Run-length and emphasis
			Run-length variability
	From grey level size zone matrices <i>They reflect regional intensity variations or the distribution of homogeneous regions</i>	Regional	Zone emphasis
			Size-zone variability
Shape and Size			Sphericity
			Compactness
			Eccentricity
			Surface Area
			Spherical Disproportion
			Surface to Volume ratio
			Solidity






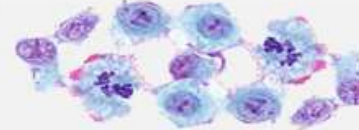

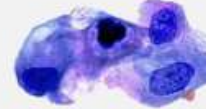


Radiomics



https://www.researchgate.net/figure/Various-radiomic-features-such-as-mesh-based-shape-histogram-gray-level-co-occurrence_fig3_315902486

Morphological features

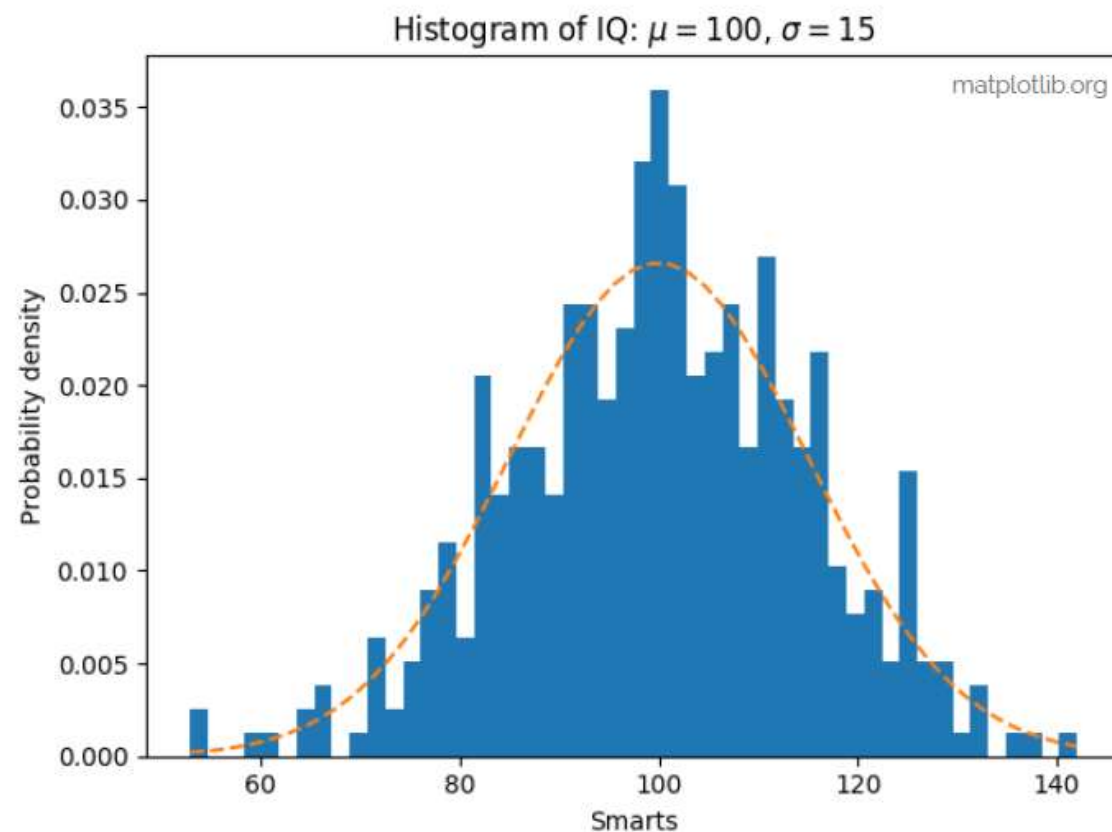
1. Metabolic Target Volume (MTV)
2. Surface
3. Spherical disproportion
(ratio between measured surface of the lesion and surface of an equivalent-sphere in terms of volume)
4. Sphericity
5. Surface-to-volume ratio

Normal	Cancer	
		Large, variably shaped nuclei
		Many dividing cells; Disorganized arrangement
		Variation in size and shape
		Loss of normal features

http://sphweb.bumc.bu.edu/otlt/MPH-Modules/PH/PH709_Cancer/PH709_Cancer7.html

Histogram-based features

1. Maximum
2. Minimum
3. Mean
4. Median
5. Mean Absolute Deviation (MAD)
6. Root Mean Square (RMS)
7. Energy
8. Entropy
9. Kurtosis
10. Skewness
11. Standard Deviation
12. Uniformity
13. Variance

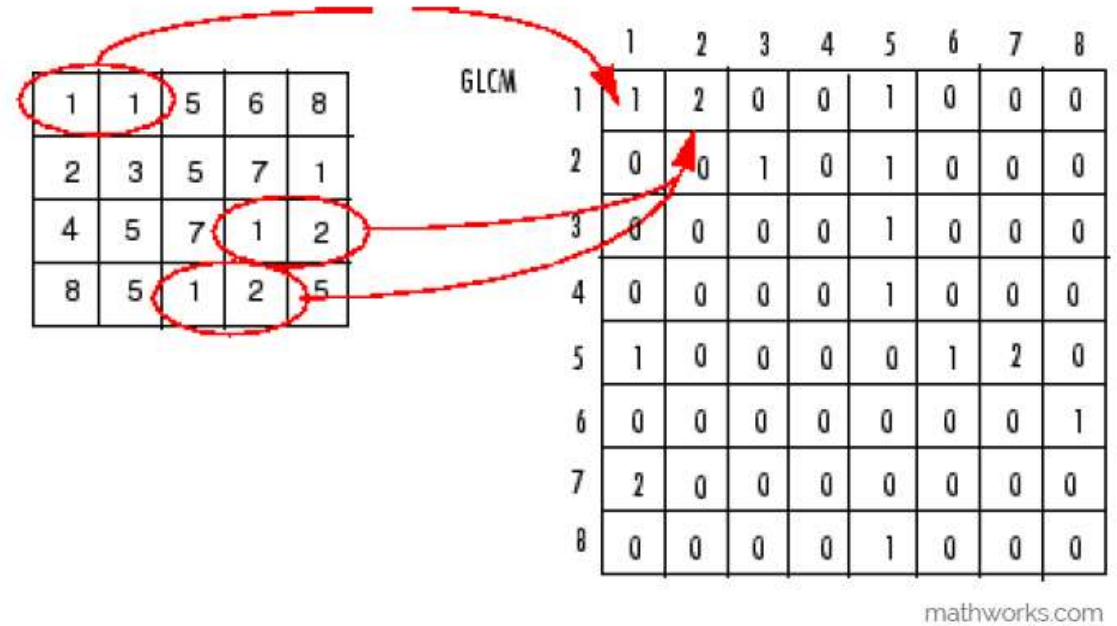


Texture descriptors

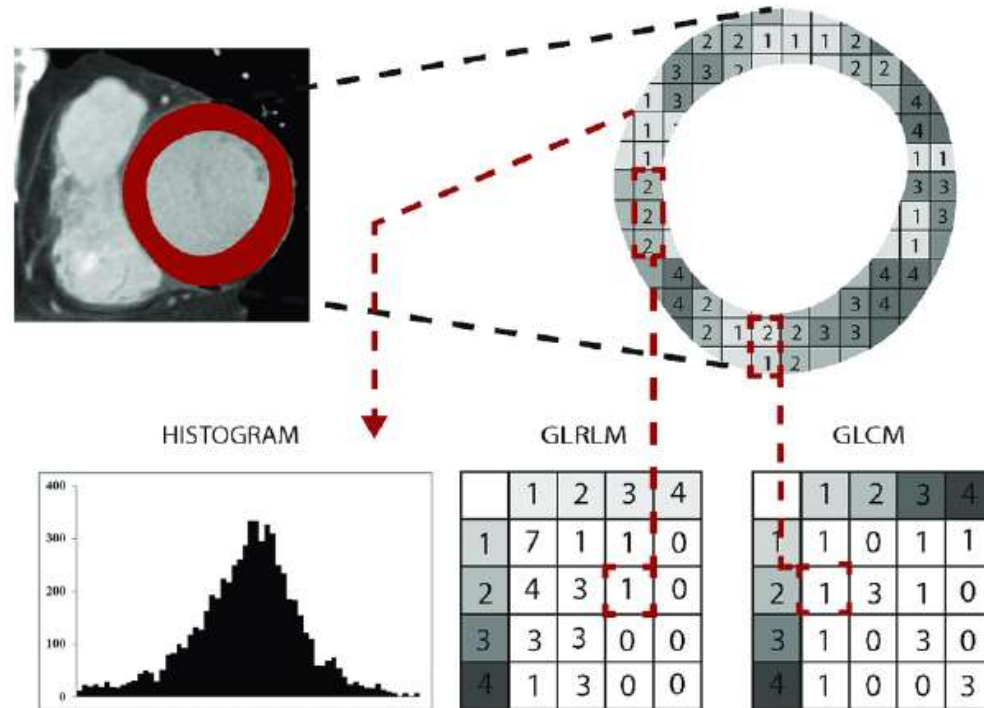
Gray-Level Co-occurrence Matrix (GLCM)*

1. Energy
2. Contrast
3. Entropy
4. Homogeneity
5. Correlation
6. Sum Average
7. Variance
8. Dissimilarity
9. Auto Correlation

* A Gray Level Co-occurrence Matrix (GLCM) quantifies the number of times the combination of levels X and Y occur in two pixels in the image that are separated by a distance of D pixels along angle A.



Texture descriptors Gray-Level Run Length Matrix (GLRLM)*



https://www.researchgate.net/figure/Principles-of-generating-texture-analysis-features-Principles-of-generating-the_fig2_320821651

*A Gray Level Run Length Matrix (GLRLM) quantifies gray level runs, which are defined as the length in number of pixels, of consecutive pixels that have the same gray level value. It describes # runs with gray level G and length L that occur in the image along angle A.

Texture descriptors

Gray-Level Size Zone Matrix (GLSZM)

1	2	3	4
1	3	4	4
3	2	2	2
4	1	4	1

<i>Level</i>	<i>Size zone, s</i>		
<i>g</i>	1	2	3
1	2	1	0
2	1	0	1
3	0	0	1
4	2	0	1

<http://thibault.biz/Research/ThibaultMatrices/GLSZM/GLSZM.html>

* A gray level zone is defined as a the number of connected voxels that share the same gray level intensity.

Contrary to GLCM and GLRLM, the GLSZM is rotation independent, with only one matrix calculated for all directions in the ROI

Texture descriptors

Neighbouring Gray Tone Difference Matrix (NGTDM)*

$$\mathbf{I} = \begin{bmatrix} 1 & 2 & 5 & 2 \\ 3 & 5 & 1 & 3 \\ 1 & 3 & 5 & 5 \\ 3 & 1 & 1 & 1 \end{bmatrix}$$

i	n_i	p_i	s_i
1	6	0.375	13.35
2	2	0.125	2.00
3	4	0.25	2.63
4	0	0.00	0.00
5	4	0.25	10.075

<https://pyradiomics.readthedocs.io/en/latest/features.html>

* A Neighbouring Gray Tone Difference Matrix quantifies the difference between a gray value and the average gray value of its neighbours within distance D

PREPROCESSING

FEATURE EXTRACTION

FEATURE SELECTION

TRAINING AND INTERNAL TESTING

EXTRACT THE FOLLOWING FEATURE FAMILIES

MORPHOLOGICAL FEATURES

- ☒ Morphology (25 features 3D or 10 features 2D)

INTENSITY-BASED FEATURES

- ☒ Intensity-based statistic (18 features)
- ☒ Intensity histogram features (16 features)

TEXTURE-BASED FEATURES

- ☒ Grey-level co-occurrence matrix (25 features)
- ☒ Grey-level run length matrix (16 features)
- ☒ Grey-level size zone matrix (15 features)
- ☒ Neighbourhood grey tone difference matrix (5 features)
- ☒ Neighbouring grey level dependence matrix (16 features)

APPLY THE FOLLOWING TRANSFORMATION FILTERS FOR FILTER-BASED FEATURES (111 features for each filter)

- ☐ Wavelet - not recommended for 2D modalities, it will greatly increase the required time (minutes instead of seconds for each image)
- ☐ Square
- ☐ Squareroot
- ☐ Logarithm
- ☐ Exponential
- ☐ Gradient
- ☐ Laplacian of gaussian (LoG)
- ☐ Local binary patterns (LBP) - the use of this filter will greatly increase the required time (minutes instead of seconds for each image)

Textures in cancer by PET

NIH Public Access

Author Manuscript

Published as final edited form as:
Pattern Recognit. 2009 June 1; 42(6): 1162–1171. doi:10.1016/j.patcog.2008.08.011.

NIH-PA Author Manuscript

Exploring feature-based approaches in PET images for predicting cancer treatment outcomes

I. El Naqa, Ph.D.^a, P. Grigsby, M.D.^a, A. Apte, M.Sc.^a, E. Kidd, M.D.^a, E. Donnelly, M.D.^a, D. Khullar, M.Sc.^a, S. Chaudhari, B.Sc.^a, D. Yang, Ph.D.^a, M. Schmitt, B.Sc.^a, Richard Laforest, Ph.D.^b, W. Thorstad, M.D.^a, and J. O. Deasy, Ph.D.^a

^aDepartment of Radiation Oncology, Washington University School of Medicine St. Louis, MO, USA

^bDepartment of Radiology, Washington University School of Medicine, St. Louis, MO, USA

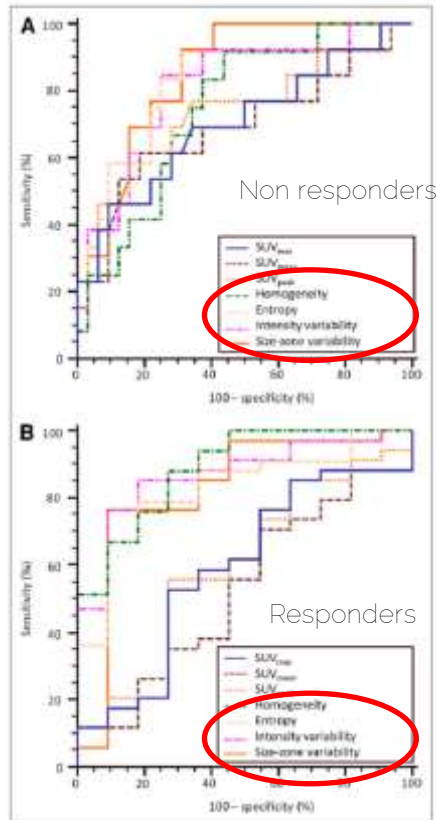


Table 2
Association between different extracted features and overall survival in a cohort of 9 head and neck patients measured by Spearman's rank correlation (rs) and the area under the ROC curve (AUC).

Variable		Spearman (rs)	AUC
Tumor volume		0.6928	0.8750
SUV Measurements	Maximum	0.3464	0.7000
	Minimum	-0.2642	0.6000
	Mean	0.1732	0.6500
	Standard deviation	0.3464	0.6750
IVH Intensity-volume metrics	I ₁₀	0.1732	0.7000
	I ₉₀	0.0	0.5000
	I ₁₀₋₉₀	0.2598	0.6750
	V ₁₀	-0.1732	0.5750
	V ₉₀	-0.7794	0.8500
	V ₁₀₋₉₀	0.0866	0.5000
Texture-based features	Energy	0.0866	0.5000
	Contrast	-0.5196	0.8000
	Local homogeneity	0.5196	0.8250
	Entropy	-0.1732	0.5250
Shape-based features	Eccentricity	0.2508	0.6500
	Euler Number	0.6266	0.8500
	Solidity	-0.6058	0.8500
	Extent	-0.6062	0.8500

J Nucl Med 2011; 52:369–378

Intratumor Heterogeneity Characterized by Textural Features on Baseline ¹⁸F-FDG PET Images Predicts Response to Concomitant Radiochemotherapy in Esophageal Cancer

Florent Tixier¹, Catherine Cheze Le Rest^{1,2}, Mathieu Hatt¹, Nidal Albarghach^{1,3}, Olivier Pradier^{1,3}, Jean-Philippe Metges^{3,4}, Laurent Corcos⁴, and Dimitris Visvikis¹

¹INSERM U650, LaTIM, CHU Morvan, Brest, France; ²Department of Nuclear Medicine, CHU Morvan, Brest, France; ³Institute of

RESEARCH ARTICLE

False Discovery Rates in PET and CT Studies with Texture Features: A Systematic Review

Anastasia Chalkidou*, Michael J. O'Doherty, Paul K. Marsden

Division of Imaging Sciences and Biomedical Engineering, Kings College London 4th Floor, Lambeth Wing, St. Thomas Hospital, SE1 7EH, London, United Kingdom

* anastasia.chalkidou@kcl.ac.uk

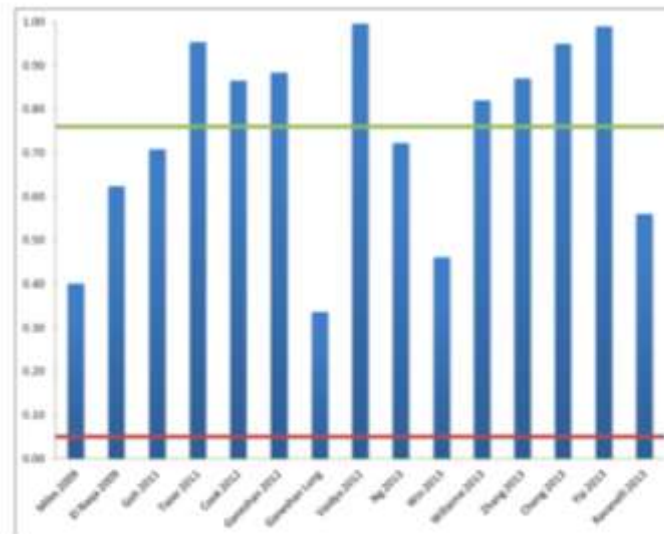


Fig 2. Probability of a false positive result based on number of hypotheses tested per study (blue columns) for all study categories. 5% type-I error probability = red line, average type-I error probability (76%) over all studies = green line (Note—additional inflation of the type-I error probability due to the use of the optimum cut-off approach is not included here).

[doi:10.1371/journal.pone.0124185.g002](https://doi.org/10.1371/journal.pone.0124185.g002)

Key methodological issues

- Repeatability, the closeness of the agreement between the results of successive radiomic measurements under the same conditions of measurement
- Reproducibility, the closeness of the agreement between the results of radiomic measurement under similar conditions of measurements
- Significance, the ability of radiomic in effectively characterizing cancer lesion heterogeneity

Stability

Biological change or radiomics instability?

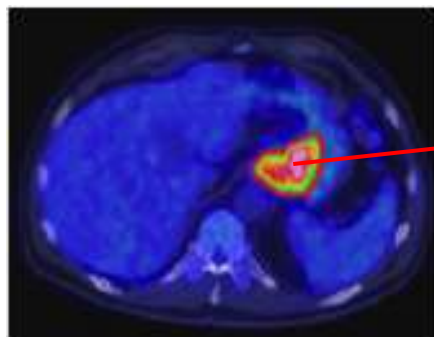
It is necessary that the radiomics features are repeatable for the same patient as part of the prognosis and therapeutic monitoring but also reproducible when performed across multiple centers and patients.

For the SUV and MTV metrics, a cut-off value of $\pm 30\%$ has been accepted for associating the changes to actual metabolic variations (PERCIST).

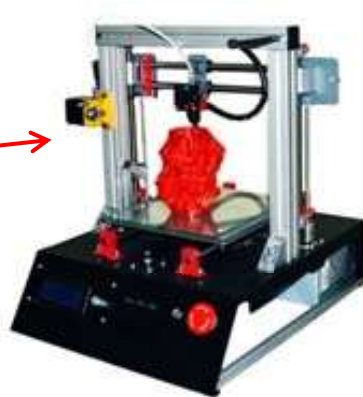
There is currently no consensus on the tolerated variability of radiomics features for the evaluation of prognosis or response to treatment.

Only radiomic features with high repeatability and reproducibility should be selected as candidate for predictive biomarkers.

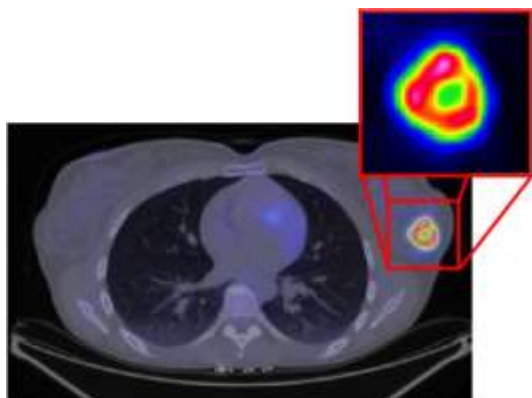
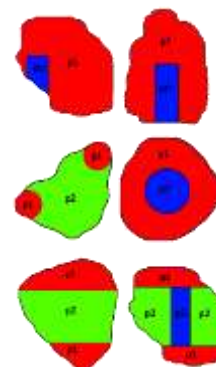
Which model to study key radiomics issues?



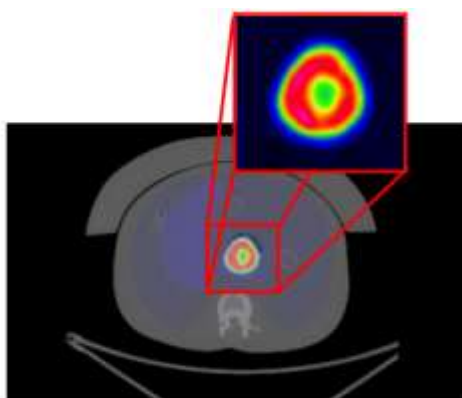
Selected as highlight at IEEE NSS MIC, Strasburgh, November 2016



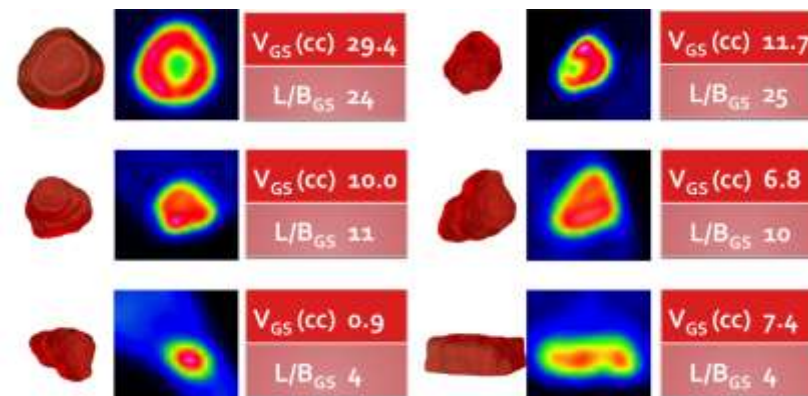
sodium
alginat
e



Real patient



Anthropomorphic phantom with syntehtic lesion



Research Article

A Method for Manufacturing Oncological Phantoms for the Quantification of 18F-FDG PET and DW-MRI Studies

Francesca Gallivanone,¹ Irene Carne,² Matteo Interlenghi,¹ Daniela D'Ambrosio,³ Maurizia Baldi,³ Daniele Fantinato,¹ and Isabella Castiglioni¹

¹Institute of Molecular Imaging and Physiology, National Research Council (IRFM-CNR), Milan, Italy

²Medical Physics Unit, IRCCS Fondazione S. Maugeri, Pavia, Italy

³Department of Diagnostic Imaging, IRCCS Fondazione S. Maugeri, Pavia, Italy

Radiomics repeatability

Medicine
Current Media & Molecular Imaging
Volume 2024, Article ID 919817, 14 pages
<https://doi.org/10.1155/2024/919817>

Research Article

Parameters Influencing PET Imaging Features: A Phantom Study with Irregular and Heterogeneous Synthetic Lesions

Francesca Gallivanone¹, Matteo Interlenghi², Daniela D'Ambrosio³,
Giuseppe Trifirò³ and Isabella Castiglioni¹

¹Institute of Molecular Imaging and Physiology, National Research Council (IFIM-CNR), Milan, Italy

²Medical Physics Unit, IRCCS Fondazione S. Maugeri, Pavia, Italy

³Nuclear Medicine Unit, IRCCS Fondazione S. Maugeri, Pavia, Italy

- Test-retest is performed among the distributions of the radiomic values obtained in the subsequent measurements.
- The pairwise Intraclass Correlation coefficient (ICC) is calculated (ICC>0.7 is considered for stability).

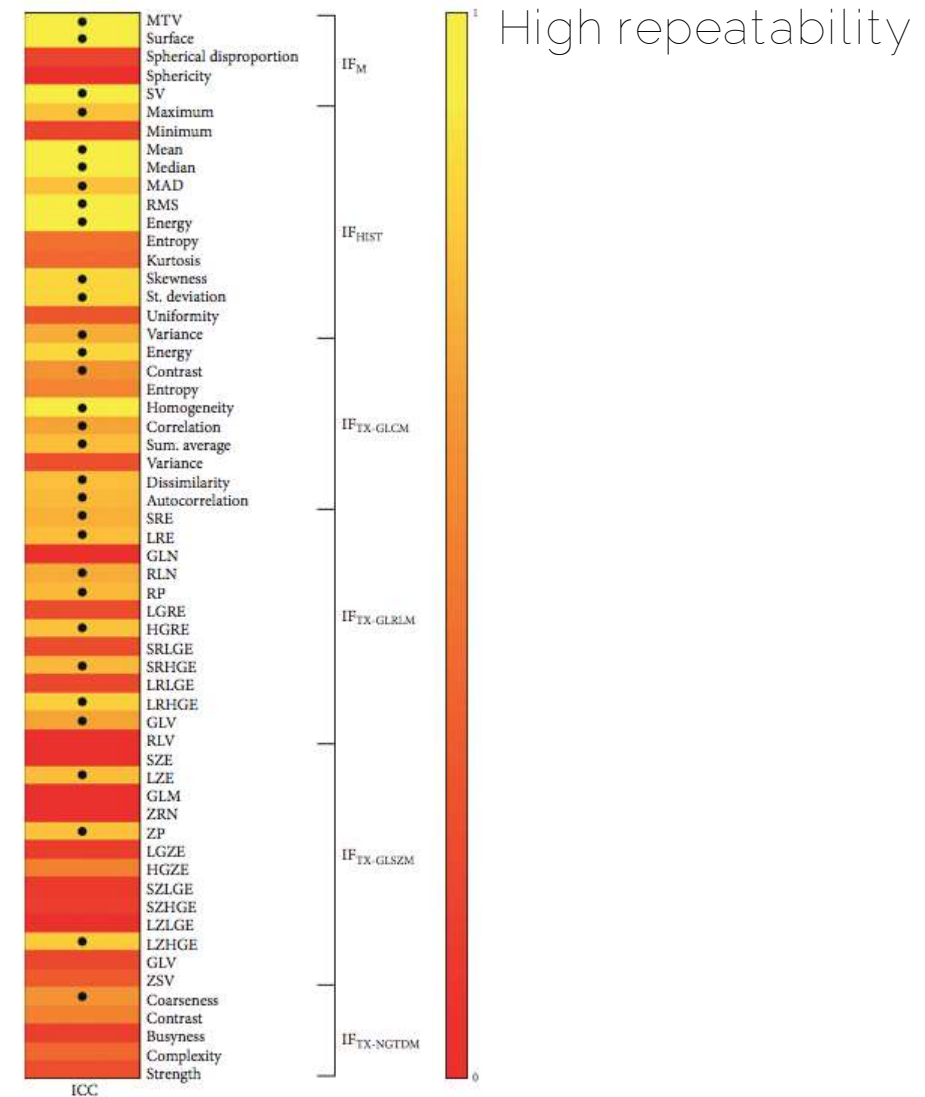


FIGURE 6: Reproducibility of radiomic features on test-retest datasets. ICC results. • indicates ICC ≥ 0.6.

Radiomics reproducibility

- Preparation
- Acquisition
- Reconstruction
- Segmentation
- Interpolation
- Re-segmentation
- Discretization

Preparation and acquisition

- Patient's conditions (e.g. Glycemia)
- Injected dose
- Scan time vs uptake time
- Time per bed position
- Respiratory motion

...

Lovat et al. 2017 – 54 neurofibromas
a significant radiomic value change between two
different uptake times both for benign and
malignant lesions

Preparation and acquisition | Respiratory motion

Vaidya et al. 2012 - 27 lung cancer

Radiomic value change considering or not respiratory motion correction by image deconvolution. *No change in radiotherapy response.*

Yip et al. 2014 - 26 lung cancer / Oliver et al. 2015 - 23 lung cancer

Radiomic value change considering or not respiratory motion correction by gating. *No results on clinical outcome.*

Grootjans et al. 2016 - 60 lung cancer

Radiomic value change in lower lobes considering or not respiratory motion correction by gating. *No change in prognosis.*

Image reconstruction

- Method (back-projection, iterative –n. it, n. subset...)
- PSF incorporation or not
- TOF incorporation or not
- Matrix size
- Filter
- PVC or not
- Statistical noise

...

Image reconstruction

Galavis et al. 2010 - 20 solid cancer

Radiomic value change with different reconstruction settings (method, n iter, matrix size, filter).

Yan et al. 2015 - 20 lung cancer / *Orlhac et al. 2017* - 54 breast cancer

Radiomic value change with different reconstruction settings (method, n iter, matrix size, filter) \pm TOF \pm PSF.

However, matrix size is the more impacting factor.

Shiri et al. 2017 - 25 lung, head, neck, liver cancer

Poor reproducibility of radiomic values for different reconstruction settings (method, n iter, n subset, matrix size, filter, PSF, TOF, scan time).

Radiomics reproducibility

MedRxiv
Coronavirus: Molecular Imaging
Volume 2020, Article ID 010017, 11 pages
<https://doi.org/10.1101/2020.03.10.2001017>

Research Article
Parameters Influencing PET Imaging Features: A Phantom Study with Irregular and Heterogeneous Synthetic Lesions

Francesca Gallivanone¹, Matteo Interlenghi¹, Daniela D'Amrosio²,
Giuseppe Trifiro³ and Isabella Castiglioni¹

¹Institute of Molecular Biomedicine and Physiology, National Research Council (IRBM-CNR), Milan, Italy
²Medical Physics Unit, IRCCS Fondazione S. Maugeri, Pavia, Italy
³Nuclear Medicine Unit, IRCCS Fondazione S. Maugeri, Pavia, Italy

Coefficient of Variation (COV) can be calculated (COV<0.10 is considered for stability)
but a statistical test is the best choice

High reproducibility

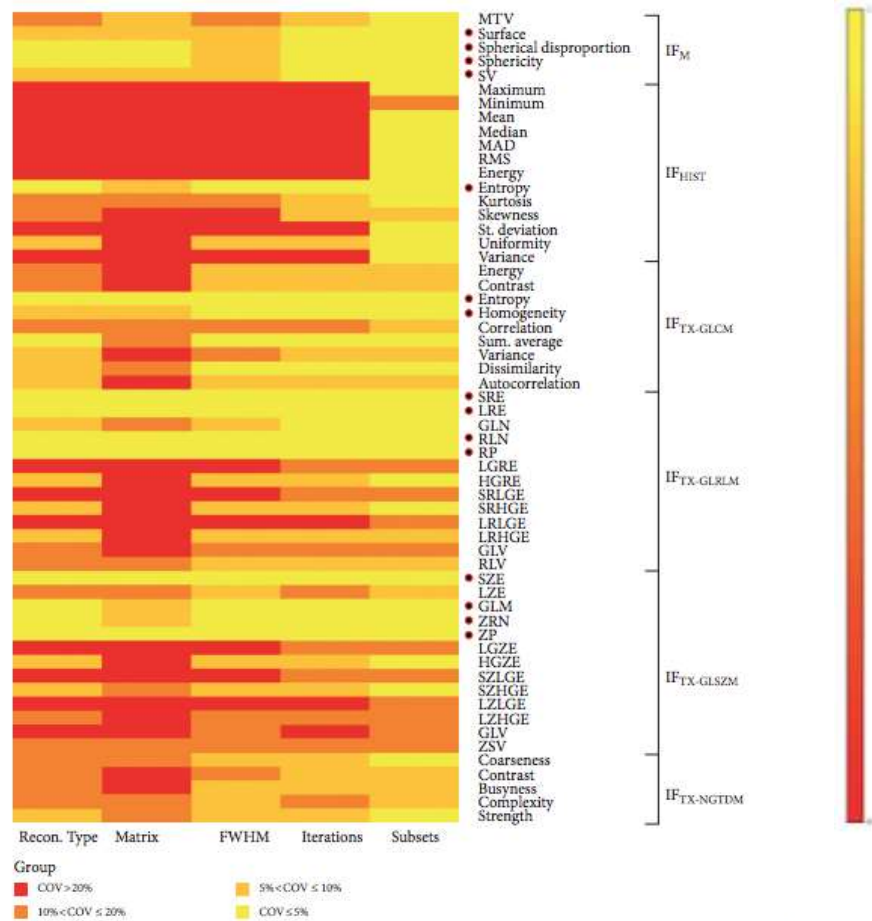
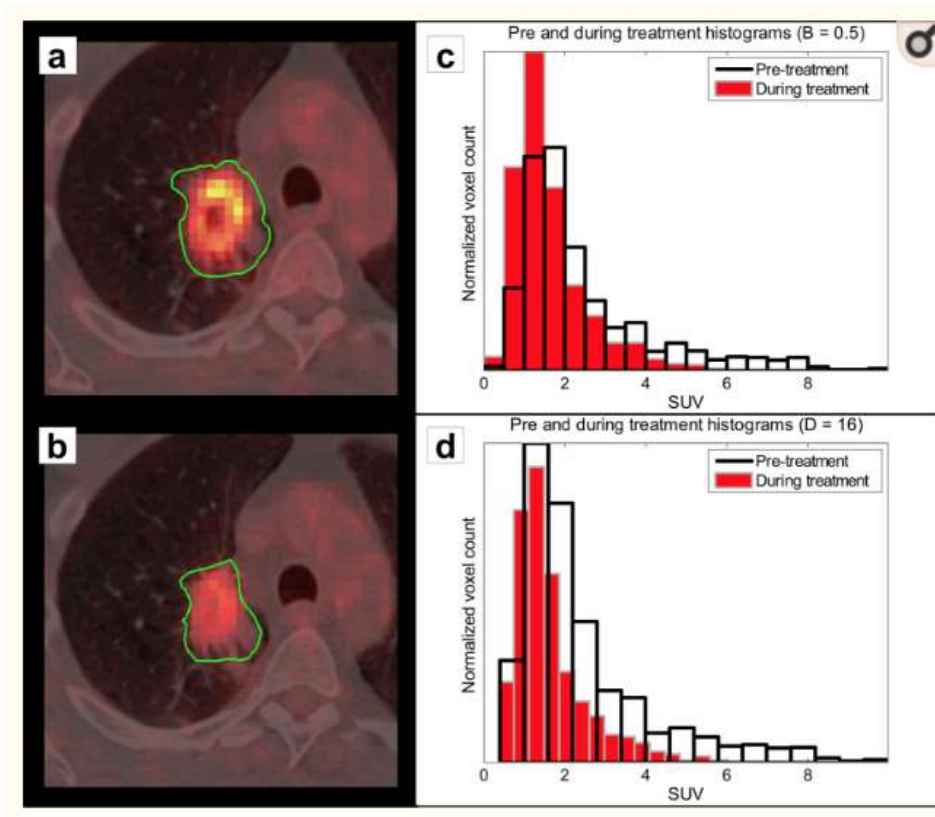


FIGURE 5: Stability of radiomic features on different reconstruction settings. COV results. • indicates COV ≤ 10%

Discretization

Resampling voxels in a limited number of intensity values (bins)
(for textural feature calculation).



Fixed bin size

Fixed bin number

Discretization

Leijenaar et al. 2015 - 35 lung cancer

Texture value is dependent on the method of discretisation
fixed bin size is recommended (constant intensity resolution,
more robust, repeatable and less sensitive to segmentation and
reconstruction changes)

Lu et al. 2016 - 40 nasopharyngeal carcinoma.

23% of texture features are stable vs fixed bin size

Orlhac et al. 2015 - 48 lung cancer & phantom studies /

Desseroit et al. 2017 - 73 lung cancer

fixed bin size is recommended (not requiring MTV of at least 45cc
but less intuitive when imaged).

Discretization

Tixier et al.2011 – 41 oesophageal cancer

Textural features are stable and less correlated with MTV for fixed bin number (64 bins is recommended since it seems to be sufficient to cover SUV range of lesions with 0.25 increments).

Segmentation

Segmentation of the tumour volume is a crucial step because all the radiomics features are calculated starting from the segmented volume.

A variety of methods exists (manual, thresholding, graph-based, region growing, statistical modelling, contour and gradient-based...)

In radiomics robustness (e.g. stability vs noise) is more important than accuracy

Segmentation

Hatt et al. 2013- 50 oesophageal cancer

Entropy, homogeneity showed moderate variability for different segmentation.
No change in radiochemotherapy response.

Leijenaar et al. 2013 - 23 lung cancer

Most textural features are stable vs4-operator manual contouring .

Orlhac et al. 2014 - 188 colorectal, lung, breast cancer

Entropy and regional textural are quite stable for different segmentation methods.

Hatt et al. 2018 - 100 lung cancer

Sphericity, homogeneity and dissimilarity value changes depending on the segmentation method

Change in prognosis and prediction of response to treatment.

Radiomics significance

MedRxiv
Coronavirus Study 2: Molecular Imaging
Volume 2020, Article ID 1110017, 11 pages
<https://doi.org/10.1101/2020.03.04.2001017>

Research Article

Parameters Influencing PET Imaging Features: A Phantom Study with Irregular and Heterogeneous Synthetic Lesions

Francesca Gallivanone¹, Matteo Interlenghi², Daniela D'Ambrosio²,
Giuseppe Trifiro³ and Isabella Castiglioni¹

¹Institute of Molecular Imaging and Physiology, National Research Council (IRCC-CNR), Milan, Italy
²Medical Physics Unit, IRCCS Fondazione S. Maugeri, Pavia, Italy
³Nuclear Medicine Unit, IRCCS Fondazione S. Maugeri, Pavia, Italy

Test correlation of radiomic features with gold-standard heterogeneity H_{GS}

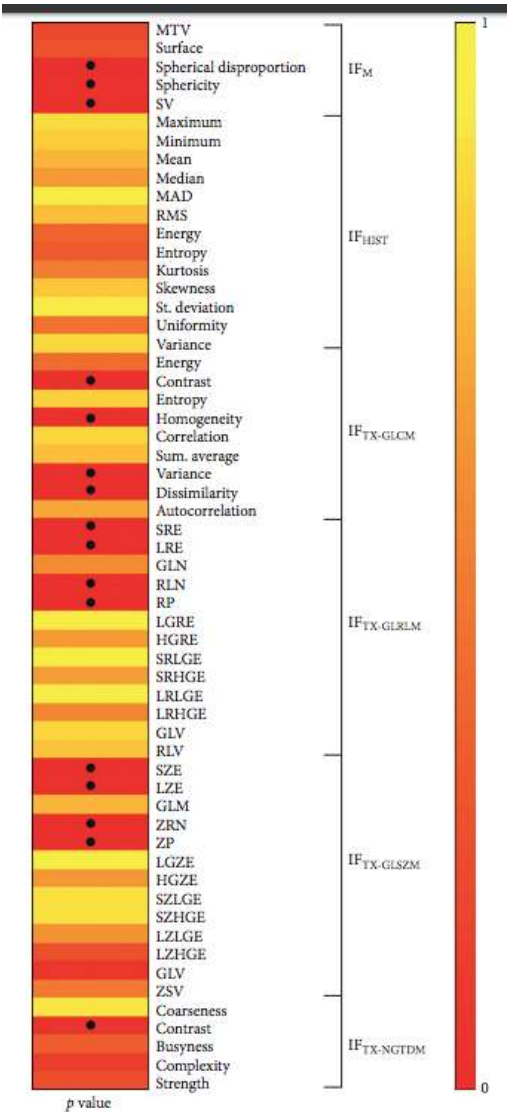


FIGURE 8: Results of correlation analysis between radiomic features and H_{GS} (p value), • indicates p value < 0.05.

High significance

Radiomics significance

MedRxiv
Coronavirus Study 2020 Molecular Imaging
Volume 2020, Article ID 1110017, 11 pages
<https://doi.org/10.1101/2020.03.04.2001017>

Research Article

Parameters Influencing PET Imaging Features: A Phantom Study with Irregular and Heterogeneous Synthetic Lesions

Francesca Gallivanone¹, Matteo Interlenghi², Daniela D'Ambrosio²,
Giuseppe Trifiro³ and Isabella Castiglioni¹

¹Institute of Molecular Imaging and Physiology, National Research Council (IRCC-CNR), Milan, Italy

²Medical Physics Unit, IRCCS Fondazione S. Maugeri, Pavia, Italy

³Nuclear Medicine Unit, IRCCS Fondazione S. Maugeri, Pavia, Italy

- test significant differences among each radiomic feature from heterogeneous vs. homogeneous uptake (e.g. Mann-Whitney test)
- measure the ability of radiomic features in discriminating heterogeneous from homogeneous lesions

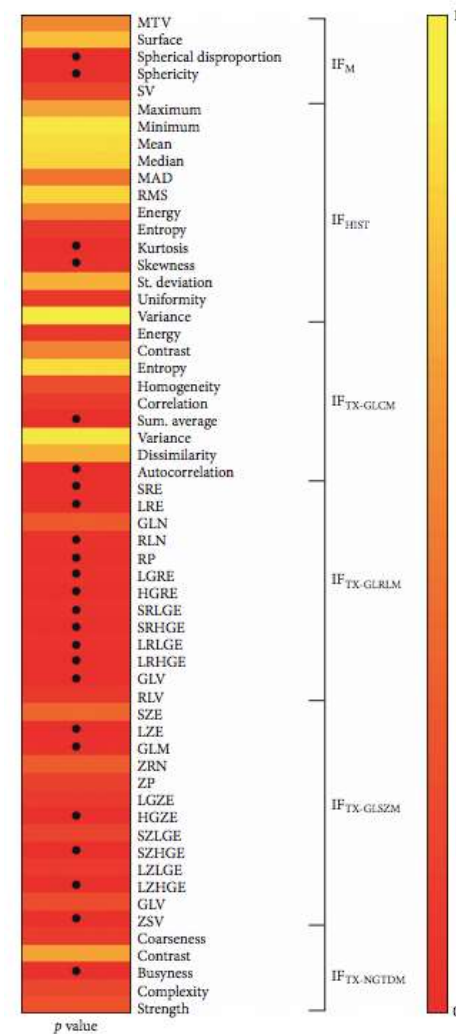


FIGURE 7: Mann-Whitney test results (p value), • indicates p value < 0.05.

High significance

Image Biomarker Standardization Initiative (IBSI)

They are providing:

- image biomarker nomenclature and definitions
- benchmark data sets and values
- reporting guidelines
- consensus-based guidelines for stable radiomic biomarkers

Zwanenburg A, Leger S, Vallières M, Löck S. Image biomarker standardisation initiative. arXiv preprint arXiv:1612.07003.

Lambin P. Radiomics Digital Phantom, CancerData (2016), DOI:10.17195/candat.2016.08.1

Image Biomarker Standardization Initiative (IBSI)

Some recommendations are delivered:
e.g. re-segmentation and discretization

Imaging intensity units ⁽¹⁾	Re-segmentation range	FBN ⁽²⁾	FBS ⁽³⁾
definite	$[a, b]$	✓	✓
	$[a, \infty)$	✓	✓
	none	✓	✗
arbitrary	none	✓	✗

Table 2.1 — Recommendations for the possible combinations of different imaging intensity definitions, re-segmentation ranges and discretisation algorithms. Checkmarks (✓) represent recommended combinations of re-segmentation range and discretisation algorithm, whereas crossmarks (✗) represent non-recommended combinations.

⁽¹⁾ PET and CT are examples of imaging modalities with *definite* intensity units (e.g. SUV and HU, respectively), and raw MRI data of arbitrary intensity units.

⁽²⁾ *Fixed bin number* (FBN) discretisation uses the actual range of intensities in the analysed ROI (re-segmented or not), and not the re-segmentation range itself (when defined).

⁽³⁾ *Fixed bin size* (FBS) discretisation uses the lower bound of the re-segmentation range as the minimum set value. When the re-segmentation range is not or cannot be defined (e.g. arbitrary intensity units), the use of the FBS algorithm is not recommended.

Working on tolerated variability of radiomics features...

A possible solution for repeatability issues



A post-reconstruction harmonization method for multicenter radiomic studies in PET

Fanny Orhac, Sarah Boughdad, Cathy Philippe, Hugo Stalla-Bourdillon, Christophe Nioche, Laurence Champion, Michaël Boussan, Frédérique Frouin, Vincent Frouin and Irène Buvat

J Nucl Med.
Published online: January 4, 2018.
DOI: 10.2967/jnumed.117.169935

Harmonization method

To pool SUV and textural features measured from different PET protocols, we tested a harmonization method previously described for genomic studies to correct the so-called batch effect. The ComBat harmonization model developed by Johnson et al (25) assumes that the value of each feature y measured in VOI j and scanner i can be written as:

$$y_{ij} = \alpha + X_{ij}\beta + \gamma_i + \delta_i \varepsilon_{ij} \quad \text{Equation 1}$$

where α is the average value for feature y , X is a design matrix for the covariates of interest, β is the vector of regression coefficients corresponding to each covariate, γ_i is the additive effect of scanner i on features supposed to follow a normal distribution, δ_i describes the multiplicative scanner effect supposed to follow an inverse gamma distribution, and ε_{ij} is an error term (normally distributed with a zero mean), as explained in Fortin et al (30). ComBat harmonization consists in estimating γ_i and δ_i using Empirical Bayes estimates (noted γ_i^* and δ_i^*) as described in (25). The normalized value of feature y for VOI j and scanner i is then obtained as:

$$y_{ij}^{\text{ComBat}} = \frac{y_{ij} - \hat{\alpha} - X_{ij}\hat{\beta} - \gamma_i^*}{\delta_i^*} + \hat{\alpha} + X_{ij}\hat{\beta} \quad \text{Equation 2}$$

where $\hat{\alpha}$ and $\hat{\beta}$ are estimators of parameters α and β respectively. The ComBat harmonization determines a transformation for each feature separately based on the batch (here Department) effect observed on feature values. In the first part of this study, we used ComBat without accounting for any biological covariate (ie $X=0$), and, in the second part, we used the TN status as the covariate of interest.

For each tissue separately (tumor and liver tissues), we applied ComBat harmonization on all features using the R function called “combat” available at <https://github.com/Hfortin/ComBatHarmonization/>.

“Centre effect” on 9 radiomic features
from breast cancer patients (63 A vs 74 B)

					After ComBat			
	TN(A) vs TN(B)	non- TN(A) vs non- TN(B)	TN(A+B) vs non- TN(A+B)	TN(B) vs non- TN(A)	TN(A) vs TN(B)	non- TN(A) vs non- TN(B)	TN(A+B) vs non- TN(A+B)	TN(B) vs non- TN(A)
Homogeneity	0.4232	0.0074	0.0014	0.4635	0.5986	0.8737	0.0015	0.0093
Entropy	0.5196	0.3906	0.0031	0.0875	0.7405	0.9139	0.0027	0.0254
SRE	0.2995	0.00044	0.0063	0.9481	0.1294	0.8338	0.0062	0.0061
LRE	0.2814	0.0004	0.0072	0.9352	0.0055	0.3871	0.0162	0.0004
LGZE	0.0405	0.0244	5.69e-05	0.3786	0.1102	0.3059	0.0002	0.0003
HGZE	0.0494	0.0282	3.20e-05	0.2886	0.2814	0.3337	2.27e-05	0.0058
SUVmax	0.0544	0.0278	7.54e-05	0.4058	0.5717	0.7943	4.47e-05	0.0072
SUVmean	0.0448	0.0359	3.20e-05	0.2394	0.4463	0.7747	3.05e-05	0.0052
SUVpeak	0.0267	0.0306	9.75e-05	0.4736	0.3581	0.7894	4.99e-05	0.0061

Table 3: P-values of Wilcoxon’s test for all features between TN and non-TN lesions from Departments A and B, before and after ComBat harmonization. Bold values are less than 0.05.

A recommendation

Test radiomic results on many
different and independent image data sets!

Radiomics: a new approach for the study of cancer



HHS Public Access
Author manuscript
Eur J Cancer. Author manuscript; available in PMC 2015 August 12.

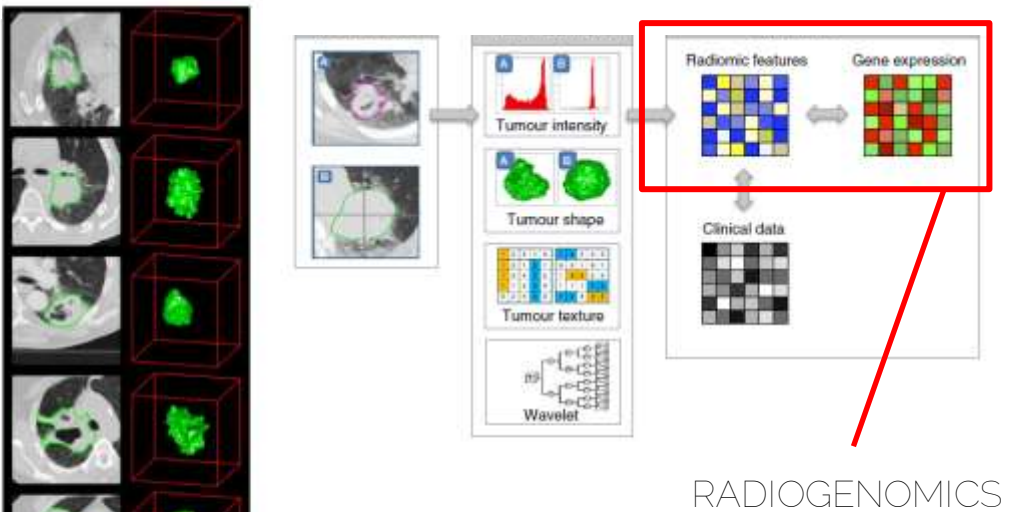
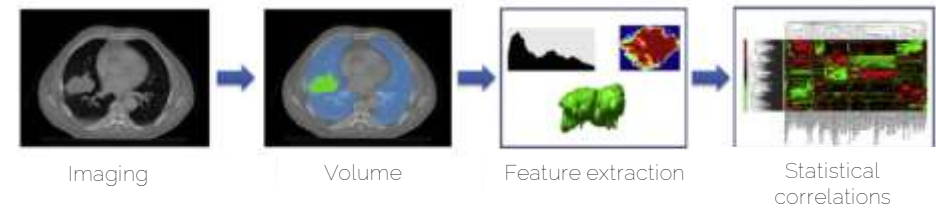
Published in final edited form as:
Eur J Cancer. 2012 March 1;48(4):441–446. doi:10.1016/j.ejca.2011.11.036.

Radiomics: Extracting more information from medical images using advanced feature analysis

Philippe Lambin^{a,*}, Emmanuel Rios-Velazquez^{a,c}, Ralph Leijenaar^{a,c}, Sara Carvalho^{a,c}, Ruud G.P.M. van Stiphout^{a,c}, Patrick Granton^{a,c}, Catharina M.L. Zegers^{a,c}, Robert Gillies^{b,e}, Ronald Boellard^{c,e}, André Dekker^{a,c}, and Hugo J.W.L. Aerts^{a,d,e}

^aDepartment of Radiation Oncology (MAASTRO), GROW – School for Oncology and Developmental Biology, Maastricht University Medical Center, Maastricht, The Netherlands ^bH. Lee Moffitt Cancer Center and Research Institute, Tampa, FL, USA ^cU University Medical Center, Department of Nuclear Medicine & PET Research, Amsterdam, The Netherlands ^dComputational Biology and Functional Genomics Laboratory, Department of Biostatistics and Computational Biology, Dana-Farber Cancer Institute, Harvard School of Public Health, USA

Comprehensive quantification of disease phenotypes by applying a large number of quantitative image features representing lesion heterogeneity and correlating with omics and clinical data



RADIOGENOMICS

CT radiogenomics for cancer

Radiology

Non-Small Cell Lung Cancer:

Identifying Prognostic Imaging Biomarkers by Leveraging Public Gene Expression Microarray Data—Methods and Preliminary Results¹

Oliver Gevaert, PhD
Jiajing Xu, MS
Chuong D. Hoang, MD
Ann N. Laung, MD
Yue Xu, PhD
Andrew Quon, MD
Daniel L. Rubin, MD, MS
Sandy Napel, PhD
Sylvia K. Plevritis, PhD

Purpose:

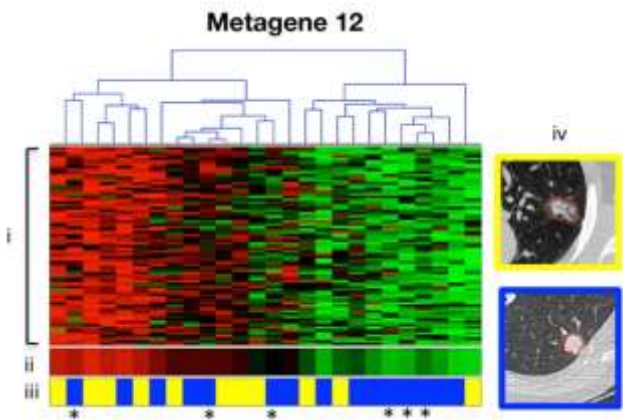
To identify prognostic imaging biomarkers in non-small cell lung cancer (NSCLC) by means of a radiogenomics strategy that integrates gene expression and medical images in patients for whom survival outcomes are not available by leveraging survival data in public gene expression data sets.

Materials and Methods:

A radiogenomics strategy for associating image features with clusters of coexpressed genes (metagenes) was defined. First, a radiogenomics correlation map is created

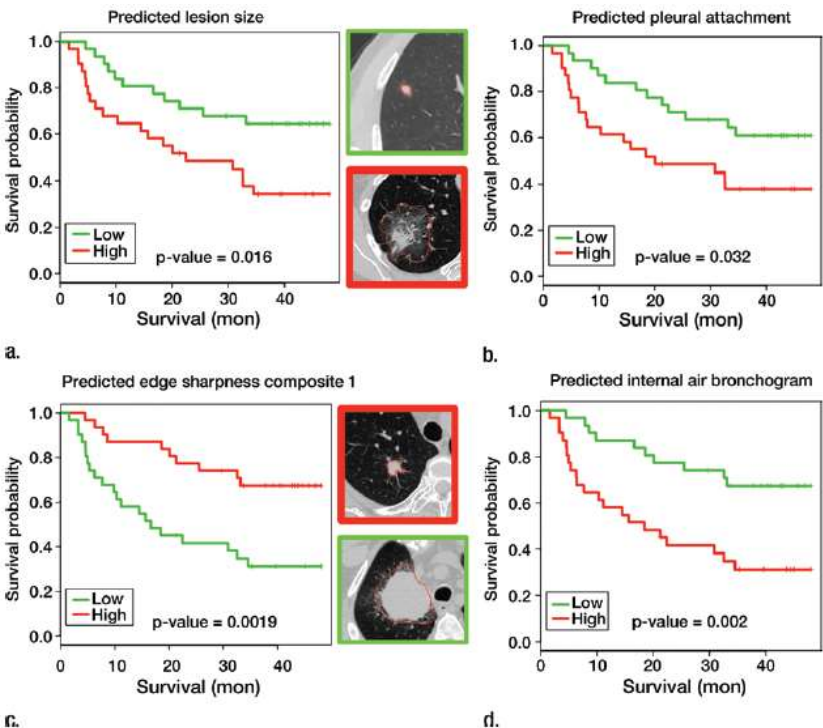
Radiology: Volume 264: Number 2—August 2012 ■ radiology.rsna.org

153 CT features



Non-Small Cell lung cancer

4 CT image features



Published online 23 December 2015

Nucleic Acids Research, 2016, Vol. 44, No. 8 e71
doi: 10.1093/nar/gkv1507

TCGAbiolinks: an R/Bioconductor package for integrative analysis of TCGA data

Antonio Colaprico^{1,2,†}, Tiago C. Silva^{3,4,†}, Catharina Olsen^{1,2}, Luciano Garofano^{5,6}, Claudia Cava⁷, Davide Garolini⁸, Thais S. Sabedot^{3,4}, Tathiane M. Malta^{3,4}, Stefano M. Pagnotta^{5,9}, Isabella Castiglioni⁷, Michele Ceccarelli¹⁰, Gianluca Bontempi^{1,2,*} and Houtan Noushmehr^{3,4,*}

¹Interuniversity Institute of Bioinformatics in Brussels (IB)², Brussels, Belgium, ²Machine Learning Group (MLG), Department d'Informatique, Université libre de Bruxelles (ULB), Brussels, Belgium, ³Department of Genetics Ribeirão Preto Medical School, University of São Paulo, Ribeirão Preto, São Paulo, Brazil, ⁴Center for Integrative Systems Biology - CISBI, NAP/USP, Ribeirão Preto, São Paulo, Brazil, ⁵Department of Science and Technology, University of Sannio, Benevento, Italy, ⁶Unlimited Software srl, Naples, Italy, ⁷Institute of Molecular Bioimaging and Physiology of the National Research Council (IBFM-CNR), Milan, Italy, ⁸Physics for Complex Systems, Department of Physics, University of Turin, Italy, ⁹Bioinformatics Laboratory, BIOGEM, Ariano Irpino, Avellino, Italy and ¹⁰Qatar Computing Research Institute (QCRI), HBKU, Doha, Qatar

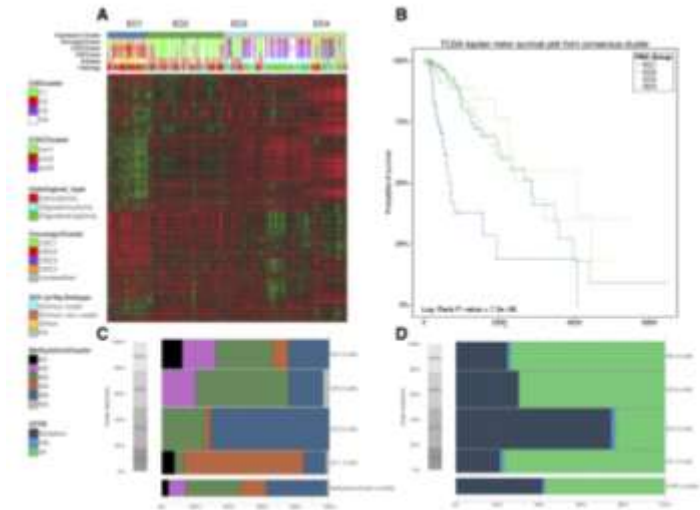


Figure 4. Case study v2.2 integrative (or downstream) analysis of gene expression and clinical data from LGG dataset with unsupervised clustering and missing expression clusters with clinical and molecular information. (A) Heatmap of 1187 non-synonymous genes clustered with tree d = 4 to EC3, EC2, EC1, EC4. (B) Kaplan-Meier survival plot for EC clusters. (C) and (D) Hierarchical clustering of the 1187 non-synonymous genes and 4785 mutations within the EC clusters.

Theranostics 2015, Vol. 5, Issue 10 1122

Theranostics

2015, 5(10): 1122-1145. doi:10.7554/theran.11245

Review

MicroRNAs: New Biomarkers for Diagnosis, Prognosis, Therapy Prediction and Therapeutic Tools for Breast Cancer

Gloria Bertoli, Claudia Cava, and Isabella Castiglioni[†]

Institute of Molecular Bioimaging and Physiology (IBFM), National Research Council (CNR), Milan, Italy

[†] Corresponding author: Institute of Molecular Bioimaging and Physiology of the National Research Council, IBFM-CNR, Via F.lli Cairo 15-20090 Segrate (MI), Italy. Email: isabella.castiglioni@ibfm.cnr.it

© 2015 Copyright International Institute for Systems Medicine. All rights reserved. No part of this publication may be reproduced, stored in a retrieval system, or transmitted, in any form or by any means, electronic, mechanical, photocopying, recording, or by any information storage or retrieval system, without prior permission in writing from the International Institute for Systems Medicine.

Received: 2015.07.09; Accepted: 2015.08.13; Published: 2015.07.14

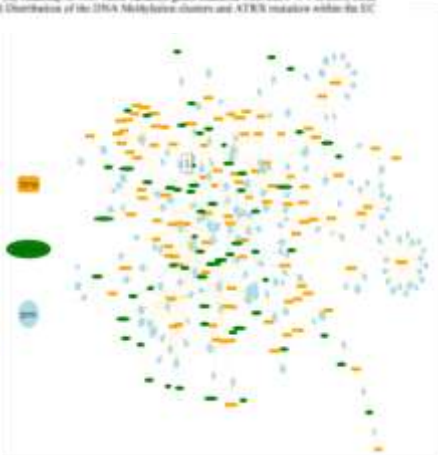
International Journal of Molecular Sciences

Article

SpidermiR: An R/Bioconductor Package for Integrative Analysis with miRNA Data

Claudia Cava^{1,*}, Antonio Colaprico^{2,3}, Gloria Bertoli¹, Alex Gradinari¹, Tiago C. Silva⁴, Catharina Olsen^{5,6}, Houtan Noushmehr^{4,5}, Gianluca Bontempi^{2,3}, Giancarlo Mauri^{6,7} and Isabella Castiglioni^{1,8}

¹ Institute of Molecular Bioimaging and Physiology National Research Council (IBFM-CNR), Segrate (MI) 20090, Italy; gloria.bertoli@ibfm.cnr.it (G.B.); alex.gradinari@ibfm.cnr.it (A.G.)
² Interuniversity Institute of Bioinformatics in Brussels (IBI), Brussels 1050, Belgium; antonio.colaprico@ulb.ac.be (A.C.); houtan@ulb.ac.be (H.N.); ghent@ulb.ac.be (G.B.)
³ Machine Learning Group (MLG), Department d'Informatique, Université libre de Bruxelles (ULB), Brussels 1050, Belgium
⁴ Department of Genetics Ribeirão Preto Medical School, University of São Paulo, Ribeirão Preto, São Paulo 14049-900, Brazil; tiagochoi@gmail.com (T.C.S.); houtan@terra.com (H.N.)
⁵ Department of Plastic Surgery, Henry Ford Hospital, Detroit, MI 48202, USA
⁶ Department of Informatics, Systems and Communication, University of Milan-Brescia, Milan 20126, Italy; mauri@ibfm.cnr.it
⁷ SYSBO Centre of Systems Biology (SYSBO), Milan 20126, Italy
⁸ Correspondence: claudia.cava@ibfm.cnr.it (C.C.); isabella.castiglioni@ibfm.cnr.it (I.C.); Tel.: +39-02-21717302 (C.C. & I.C.)



LIMINAL A	LIMINAL B	BASAL	HERE
REACTIONS degradation of the extracellular matrix	K000 amylogenesis right ventricular cardiomyopathy and	REACTIONS nerve sprouting	REACTIONS activation of the nerve axon binding of the cell binding complex and axon subsequent binding to Aβ
BIOCARTA nitrous pathway	REACTIONS urease in serine signaling	REACTIONS activation of the pre-replicative complex	REACTIONS unfolded protein response
REACTIONS also family proteins mediated transport	BIOCARTA substrate pathway	K000 sphingosine	REACTIONS developmental biology
REACTIONS ethanol oxidation	K000 threonine	K000 sphingosine	K000 other lipid metabolism
BIOCARTA amino pathway	REACTIONS cell junction organization	REACTIONS activation of an in response to receptor stress	REACTIONS peer guidance
REACTIONS metabolism of carbohydrates	K000 dna replication		REACTIONS modulates the damage response
REACTIONS glycosaminoglycan biosynthesis	REACTIONS interferon alpha beta signaling		REACTIONS aging effects
REACTIONS pleiotic activation signaling and regulation	BIOCARTA nerve pathway		REACTIONS light signal binding and activation
K000 cholesterol signaling pathway	K000 type-2 diabetes mellitus		REACTIONS phospholipase 2 mediated cascade
BIOCARTA anion pathway	BIOCARTA gl pathway		REACTIONS glycolysis
BIOCARTA longevity pathway	K000 insulin cancer		K000 histidine metabolism
REACTIONS myofibrils biosynthesis	REACTIONS a phase		K000 sulfate sulfur cell mediated substrate
REACTIONS transmembrane transport of small molecules	REACTIONS g1 a transition		REACTIONS ascorbic acid linked glycosylation
BIOCARTA ally pathway	REACTIONS amino acid synthesis and nitroreduction-hydroxylation		REACTIONS ally reactions
REACTIONS a linked glycosylation of insulin	REACTIONS metabolism of amino acids and serine		REACTIONS hematin sulfate hemoglobin metabolism
REACTIONS transport of glucose and other sugars like salts and organic acids and amino compounds	K000 arginine and proline metabolism		K000 melanoma
REACTIONS factors involved in megakaryocyte development and platelet production	K000 glycolysis gluconeogenesis		
	BIOCARTA rxn pathway		
	REACTIONS extension of telomeres		

Conclusions

Radiomic features have been shown to be sensitive to many factors, i.e. preparation & acquisition, reconstruction, segmentation and new ones, more specific of radiomic (e.g discretization).

Factors not only influence the values of radiomics but their extent is highly variable with different results.

These instability generate fluctuations that should not be misinterpreted as being of biological meaning.

Conclusions

Some solutions are coming and collecting from research groups involved in radiomic harmonization initiatives (e.g. IBSI)

Until clear recommendations on how to harmonize data are defined, you should select only highly repeatable and reproducible radiomic features from your clinical imaging studies and validate in independent studies to select candidates radiomic biomarkers for prognosis and prediction.

However, it is currently not possible to formally exclude any radiomics feature from future investigations solely based upon their low repeatability and reproducibility.

Conclusions

Advanced image processing such as radiomics combined with machine learning can develop models based on imaging signatures for predicting phenotype subtype prognosis and response to therapy

They are opening new role to in-vivo medical imaging in predictive personalized medicine

Some radiomic methodological issues (e.g. lesion segmentation, feature harmonization and stability) need robust solutions and validations prior to be translated in clinical studies

Radiomic predicting models can be improved by liquid epigenomics for integrated phenotype models